EFFECTIVE STRATEGY FOR PHOTOGRAMMETRIC 3D MODELS IN CASE OF EMERGENCIES

S. Gagliolo [a], R. Fagandini[b], D. Passoni[a], B. Federici[a], I. Ferrando[a], D. Pagliari[b], L. Pinto[b], D. Sguerso[a]

[a] Università degli Studi di Genova, DICCA – Laboratory of Geodesy, Geomatics and GIS, Via Montallegro 1, 16145 Genoa
(sara.gagliolo, ilaria.ferrando)@edu.unige.it, daniele.passoni@dicca.unige.it, (bianca.federici, domenico.sguerso)@unige.it
[b] Politecnico di Milano, DICA – Geodesy and Geomatics section, Piazza L. da Vinci 32, 20133 Milan
(roberta.fagandini, diana.pagliari, livio.pinto)@polimi.it

KEY WORDS: UAS, Photogrammetry, Emergency, Survey strategy, Cultural Heritage, Safety, Optimization

ABSTRACT:

An optimized survey planning and realization, coupled with well thought out processing, allows obtaining good quality results, guaranteeing at the same time a reasonable use of resources and time. In fact, a well-organized survey represents a benefit for both operators and end-users. The former can save time and acquire smaller datasets to be processed, while the latter can invest their resources better. These goals are even more important in case of emergencies, because the situation can quickly change, causing risk for both people and goods. The paper examines the possibility of using Unmanned Aerial Systems (UAS) photogrammetry for 3D modelling in case of emergencies, focusing on finding a trade-off between the final accuracy and the requested processing time. An experimental test has been conducted over the Castle of Casalbagliano, a damaged structure located near Alessandria (Northern Italy). Different processing strategies have been tested to define useful guidelines and recommendations to be used in emergencies scenarios. The quality of the different processing has been evaluated both in terms of residuals on the bundle block adjustment and quality of the generated dense point cloud, which has been compared with a Terrestrial Laser Scanner (TLS) point cloud. Finally, the possibility of Web publication of the produced 3D models has been exploited too.

1. INTRODUCTION

In case a catastrophic event damages an area, several aspects need to be taken into account. The first and main goal is to save human lives; in facts, the most urgent actions are intended to help people to step back from danger. Then, the second important aim is the conservation of goods. This paper has been developed focusing on this second aspect, paying particular attention to the preservation of cultural and artistic heritage (e.g. buildings).

The interest of researchers on cultural heritage documentation and their 3D modelling has widespread in the last decades, focusing on different aspects: from pure historical image documentation (Yastikli, 2007; Yilmaz, 2007), mapping (Remondino, 2011), digital reconstruction of destroyed objects (Grün et al., 2004) to the creation of Web-catalogues and virtual museum tours (Wojciechowski, 2004; Bruno et al., 2010). Moreover, cultural heritage 3D models could help in securing, planning and performing the restoration of damaged buildings. Considering this last task, UAS photogrammetry can guarantee the metrical precision of the results, facilitating at the same time the access in areas where otherwise it would be impossible to enter. Furthermore, the used instrumentation by this technique is cheap and the survey operations are quick. Hence, its use is very common and there is a plenty of applications spacing in different fields (e.g. for architectural applications see for instance Themistocleous, 2015; Sauerbier and Eisenbeiss, 2010; Brutto et al., 2014).

The UAS photogrammetry features could be very helpful in emergency situations (e.g. earthquakes), when a high level of precision and accuracy is required to ensure building conservation, as well as preserving their cultural value.

The use of UAS for post-emergencies events and their integration with different surveying methods has been exploited by a number of authors (see for instance Xu, 2014; Achille et al., 2015; Meyer et al., 2015; Ballarin et al., 2013; Gagliolo et al., 2017).

The main goal of the work discussed in the present paper is to create a step-by-step operative workflow that could be used in a fast and simple way for generating different photogrammetric products (namely dense point clouds and orthophotos). Moreover, the photogrammetric products could be published on the Web, ensuring to them a worldwide distribution and an easiness of access, e.g. allowing performing quick interrogations and accurate measurements. Such products could help also the local authority and/or Civil Defense to secure the site faster, using fewer resources and making the operations more effective.

To simulate an emergency scenario and to face the real difficulties imposed by such context, the ruins of a castle were chosen as case study. Of course, in case of real applications, it is mandatory to take into account the specific conditions of the surveyed area and carry on a deep analysis on site. The present work is intended as a collection of guidelines to support the operators in the choice of the best strategy to apply for photogrammetric flight and data processing, dense cloud generation and web pubblication.

The dissertation is organized as follows: in Section 2 the selected test area, the planning and the realization of the photogrammetric flights are presented. Few hints about the photogrammetric data processing in different scenarios and the estimated precision are briefly described (for more details refer to Gagliolo et al., 2017).

Section 3 focuses on dense cloud generation and on the computational time requested.

In Section 4, the procedure to share on a Web platform the created models, with the aim to give to end-users the instruments for performing simple analysis (e.g. the extraction of sections or distance measurements), is shown. This is an important resource for simplifying the end-users

interaction with the models, enhancing at the same time the work done.
Final considerations and future proposals are discussed in Section 5.

2. PREVIOUS EXPERIENCES IN THE TEST AREA

2.1 Case study

The analysed case study is the Castle of Casalbagliano, located in the countryside of Alessandria (Piedmont, Italy) (see Fig. 1). The castle was built at the end of XIII century by the Bagliani's lineage. The toponym has been recently attributed in memory of the founder family.

Figure 1. Castle of Casalbagliano

2.2 Survey campaign

The investigated area has been object of a preliminary inspection, to carefully plan the data acquisition. Then, the survey campaign was carried out in a single day.
The survey has been realized testing different acquisition techniques to compare the final metric accuracy. Total Station (Leica Nova MS60 Multistation; MS) and GPS (Topcon Hiper Pro) were used to measure the coordinates of the Ground Control Points (GCPs), while UAS Photogrammetry and TLS (Z+F Imager® 5006h) were used to survey the object. For more details about the survey planning, the data acquisition and the quality of the processed photogrammetric blocks (in terms of residuals on the Check Points), see Gagliolo et al. (2017).
Concerning the photogrammetric survey, the images have been captured using a Canon EOS-M camera, with a fixed focal length equal to 22 mm. Three different data sets have been acquired; for the first and the second one the camera has been installed on a Microcopter hexacopter, which is equipped with an on board low-cost GNSS receiver (Ublox LEA GH), a triaxial magnetometer and a Micro Electro-Mechanical System/Inertial Measurement Unit (MEMS/IMU). Its maximum payload is about 0.5 kg and it has a flight autonomy of about 15 min. The third data set has been acquired using terrestrial photogrammetry.
The average flight height for the first nadir dataset was about 40 m. The flight has been planned to guarantee a high overlapping (80% along flight direction and 70% along cross direction), resulting in an average Ground Sample Distance (GSD) of about 9 mm.
The second flight was realized using an oblique camera configuration (tilt angle equal to 45°), describing a square around the castle, maintaining a fixed distance of about 50 m. In this case, the flight height has been set equal to 50 m, guaranteeing an overlapping of about 80%.

2.3 Ground Control Points

The photogrammetric block has been georeferenced using 19 GCPs, materialized using black and white square targets (0.3 m side), which have been divided into three different groups (see Fig. 2). For all the considered scenarios, four points have been used as Check Points (CPs), to evaluate the quality of the bundle block adjustment. Both MS and TLS have been located in eight station points, as shown in Fig. 3.

Figure 2. Locations of the GCPs and CPs over the surveyed area. The blue squares represent the 4 CPs. The 15 GCPs of first test case are reported in red and green, the 12 GCPs of the second test case are depicted in green and the 3 GCPs of the third test case are represented by stars

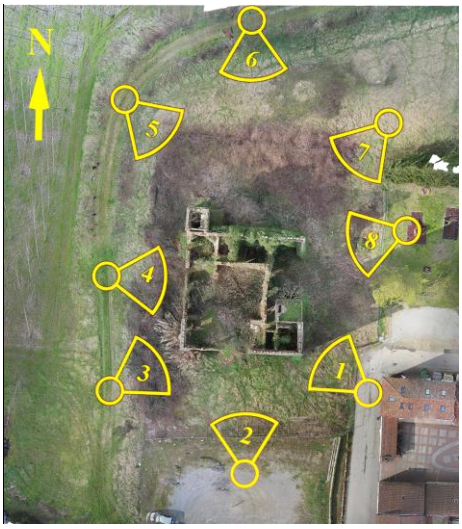

Figure 3. Locations of station points used for the laser scanner acquisition and for the determination of the geodetic network

The used MS is characterized by an angular accuracy of 3^{cc} and by a distance accuracy of 1 mm + 1.5 ppm (using reflective prism), when it is used in Total Station mode (Fagandini et al., 2017). The local reference system has been defined with its origin in the point 1, the y-axis oriented

towards point 8 (i.e. parallel to one of the perimeter walls), the z-axis oriented along the vertical and the x-axis to complete the right-handed Cartesian reference frame. The geodetic network has been adjusted using the Infinity software, supplied by the MS manufacturer, resulting in a closing angle error of 50^{cc}. The target coordinates have been measured with both MS and GNSS (NRTK mode), reaching an accuracy of 0.02 m. The TLS scans have been realised using a resolution of 20,000 points/360°, guaranteeing a spacing of about 0.01 m in the acquired point clouds. In order to align the different scans, 32 Forex reflective black and white targets have been arranged in the surveyed area. This was necessary despite of the presence of photogrammetric GCPs, because of the impossibility to see them clearly in the TLS scans.
The targets have been placed on different objects located around the scene (e.g. perimeter fences, trees etc.), distributed along any direction, ensuring better results in the scans alignment phase. The coordinates of these targets have been measured with the MS, maintaining the highest possible redundancy, and adjusted in the geodetic network.
Finally, additional scans have been performed using the MS, stationing on the same points used for the realisation of the geodetic network (see Fig. 3).

2.4 Data processing

All the acquired photogrammetric blocks have been processed with the commercial software Agisoft Photoscan - version 1.2.6 (http://www.agisoft.com/), using the standard workflow proposed by the software itself. All the analysis discussed in the present paper have been carried out using a desktop Personal Computer (64 bits Windows 7 operating system, Intel® core™ ¡7-4770 CPU @340 GHz processor and 32 GB of RAM, Intel® HD Graphics 4600, 20 Cores @400 MHz, 1297 MB). After the solution of the bundle-block adjustment and the estimation of External Orientation (EO) parameters, the self-calibration has been performed through the 'Optimize Cameras' option (for all the considered scenarios). In fact, it is quite important to refine the Internal Orientation (IO) parameters in case of UAS flights, because they can easily be subject to variations due to the impacts suffered by the lens during take-off and landing.
Different configurations and constraints for image processing have been considered for the discussed tests. The results have been evaluated in terms of final accuracy and computational cost. The acquired images have been divided into three groups, relying on the specific acquisition geometry: nadir images (83 frames; N), oblique images (61 frames; O) and terrestrial acquisition (28 frames; T). It is worth to notice that it is possible to fully reconstruct the whole structure only using the O dataset. Indeed, the N and T images do not give a complete view of the object, because they focus on a preferential portion (roofs and façades, respectively); thus it is not possible to realize a complete model using just these two datasets.
A second variable taken into account was the number and the distribution of GCPs, focusing on three different configurations. For all the considered scenarios, the same dataset of CPs has been used to evaluate the quality of the photogrammetric solution (see blue squares in Fig. 2). The CPs locations have been set to obtain a quite regular distribution around the investigated structure. It is worth to notice that the structure is not accessible, thus the targets could not be located in the internal area.
In the first case, the whole set of 15 GCPs was used; in the second scenario, 12 GCPs were selected from the previous one, discarding the worst points; finally, the third scenario involved the minimum number of requested GCPs (3).
The impact of the image resolution on EO parameters estimation has been evaluated. Two different scenarios were analysed, respectively the use of images at their full resolution (H) and their downscaling by a factor 4 (i.e. 2 times for each side; M).
Different processing have been tested, combining the three datasets of images. It is important to point out that adding images to the O dataset (taken from N or T) does not implicate any specific improvement, mainly because the oblique geometry was already auto-consistent, thanks to a rigorous planning, thus guaranteeing a high overlapping and the completeness of the final model.
The overall quality of the bundle block adjustment obtained in Gagliolo et al. (2017) resulted in about 0.03 m for all the considered scenarios.

3. OPERATIVE STRATEGY

The main purpose of the discussed analysis is the optimization of the survey phases, in order to obtain only the necessary products as quickly as possible, respecting the required precisions. The prospected scenario is a situation of emergency, which might be rapidly solved, with the use of a restrained set of resources and ensuring the operators' safety.

3.1 Objective definition

The objectives of the photogrammetric survey are summarized in the following list: (1) detection of the building in its context; (2) acquisition of the volume of the entire object and eventually (3) of the ruins to remove or restore; (4) inspection of any historical-artistic-architectural presences to preserve them. These requirements need different levels of deepen and different resolutions and densities of the dense clouds.
The influence of the image resolution has been considered, for each block geometry and constraint, by using different 'alignment' quality values of the Photoscan software.
The quality of the computed solution has been evaluated by considering the Root Mean Square Errors (RMSE) of the CPs. The RMSE are below 0.03 m for all acquisition geometries and considered GCPs configurations. The case with 3 GCPs was considered for simulating a critical situation (e.g. operator's difficulties in measuring GCPs because of the presence of ruins). Nevertheless, even in this case, the results show that the influence of the photogrammetric block geometry on the quality was negligible if compared to the accuracy requested in case of an emergency survey. This is probably because the block geometry of the O case was already consistent, thanks also to the high overlapping. The requested time for processing the image datasets is strictly connected to the number of frames that compose the photogrammetric block and to the availability of image geo-location (position and attitude), useful for image pair pre-selection. However, for the analysed scenario, none of this information was available.
The different amount of time request for the EO processing, considering H o M image quality, is about 30%, which could be considered tolerable if the total computational time does not exceed one-hour limit. Therefore, the authors recommend choosing the block configuration considering both the complexity of the object, its texture and the available time for delivering results. In fact, if it is necessary to give instantaneous information for safety works, a medium quality

is suggested for immediately processing the dataset on-site. On the other hand, a high quality is recommended when it is possible to process the data in laboratory. In this second case, a maximum processing time of half a day should be considered. The dense clouds have been generated only for those cases considered significant in terms of EO results. Also in this case, different quality levels have been considered, as better detailed in following paragraph 3.2.

3.2 Dense cloud time processing analysis

In this paragraph, the influence of image quality on the processing time (for both EO and dense cloud generation) is addressed, focusing on the impact of block geometry and GCPs distribution too.
Table 1 reports the different block geometries for which the dense clouds have been computed, together with the time request to produce the results and the number of generated points.

Block geom.	Nr. GCP	Quality (EO)	Quality (Dense Cloud)	Time (h:m)	Nr. of points (10^6)
N+O+T	15	H	H	29:58	41.7
N+O	15	H	H	30:14	42.6
N+O	15	H	M	4:15	15.1
O	15	M	H	8:15	28.3
O	15	M	M	1:11	7.4
O	15	H	H	11:07	28.4
O	15	H	M	1:30	7.7
O	12	M	H	8:21	30.2
O	12	M	M	1:09	7.9
O	12	H	H	11:28	29.1
O	12	H	M	1:35	7.5
O	3	M	H	8:31	29.1
O	3	M	M	1:10	7.6
O	3	H	H	11:19	28.0
O	3	H	M	1:34	7.8

Table 1. Processing times and number of points for each tested scenario

Obviously, the requested time for processing N+O+T and N+O is higher, with respect to O case. Furthermore, as already mentioned, the addition of images cannot be appreciated because the O case was already auto-consistent. However, the number of generated points is higher for N+O+T and N+O, because of the presence of multiple points of view.
The analysis of the O case shows that the image quality selected for the EO phase influences the time requested for the dense cloud generation; nevertheless, the number of points that compose the dense clouds does not change. Furthermore, no impact connected to the number of GCPs has been registered.
The dimension of the point clouds generated using H is about four times higher than the ones generated using M, according to the downscaling factor applied to the images.
It is worth to notice that the absolute requested time for image processing is strictly connected to the used hardware and the specific processed dataset. However, general information about the impact of the different parameters can be deduced, in spite of the employed software is not an open source software, thus the embedded algorithms are unknown.
Comparing the M and H solutions on quality, the former requires 1/7 of the computational time of the latter, and it produces 1/4 of the points. These differences are substantial in case of emergency and they influence the choice of the processing parameters.
Comparing the solutions obtained using the same dense cloud quality but different EO image resolutions (M vs H 'alignment'), the computational time increases of about 20%, which can be considered tolerable to obtain higher precision.
Concerning the dense cloud generation phase, an emergency scenario makes the use of medium quality preferable; in fact, the high quality setting requires a computational time which results excessive to obtain an immediate solution on site, but also for performing a fast processing in laboratory.
Moreover, it is also evident that the total computational time is still too long in case of an on-site elaboration; even considering M quality for both EO and dense cloud computation (about two hours or more).
For all these reasons, another combination has been tested, setting the low quality (L) for the dense cloud generation. This analysis has been carried out only for the O case, using 15 GCPs and an H quality alignment.
The results are summarized in Table 2.

Block geom.	Nr. GCP	Quality (EO)	Quality (Dense Cloud)	Time (h:m)	Nr. of points (10^6)
O	15	H	H	11:07	28.4
O	15	H	M	1:30	7.7
O	15	H	L	0:15	1.9

Table 2. Processing time and number of points for the combinations with only O images, 15 GCPs, high quality EO and different dense cloud quality

For the L solution, the requested computational time is about the 20% of the one for M and even the 2% of the one with H quality. In this case, the appropriate speed for the operations on site is clearly guaranteed, resulting in a detriment of the resolution of the generated point cloud.
Of course, a unique level of detail cannot be sufficient to meet all the stakeholders' requirements, especially if high-resolution results are needed. In order to pursue the optimal processing strategy, it is important to answer to two main questions: (1) What are the point clouds density variations between M and H quality? (2) What is the proper image quality to be selected in order to reach the different resolution scales needed to describe the object, its architectonical details and its relation with the context?
Therefore, the proposal is to diversify the processing, focusing on the satisfaction of the single stakeholder, thus identifying the most appropriate processing quality. In this way, it is possible to avoid the worthless processing (e.g. excessive high quality), resulting in a saving of time. Of course, such diversification requires a substantial knowledge of the photogrammetric problem and of the software characteristics by the operator, whose work could not be limited to the launch of the different phases that compose a standard processing workflow.
For this last part of the discussed analysis, only the O image dataset has been used, selecting 15 GCPs and H EO quality. The aim of the analysis discussed in the following paragraph 3.4 is to evaluate the quality of the dense clouds in terms of their density. This task could be very useful for defining the best strategy to be followed, according to the desired levels of detail. Finally, a comparison with TLS is performed to validate the photogrammetric products.

3.3 Point clouds density

The density of the dense clouds has been evaluated considering the number of points in about a square meter. Six samples were taken into account in different areas of the Castle façades, at different heights as shown in Fig.4, Fig. 5, Fig. 6. Fig. 7.

Figure 4. Samples on West façade

Figure 5. Sample on North façade

Figure 6. Sample on East façade

Figure 7. Samples on South façade

In Table 3, for each of the samples that have been taken into account, the number of points per square meter and the space between them are reported. There are no significant differences among the considered samples.

	Points per m²			**Linear space between points (cm)**		
Sample origin	L	M	H	L	M	H
W 1	144	529	2057	8.3	4.3	2.2
W 2	132	552	2127	8.7	4.3	2.2
N	128	474	1343	8.8	4.6	2.7
E	145	554	2148	8.3	4.2	2.2
S 1	128	591	2292	8.8	4.1	2.1
S 2	160	836	3233	7.9	3.5	1.8

Table 3. Density of the considered samples on the Castle's façades

From Table 3, considering a GSD of 9 mm, in L the spacing between points is about 9-10 times the GSD, in M it is about 4-5 times the GSD, while in H it is 2-3 times the GSD.
The case with UltraHigh quality (UH) was performed only considering the tower, because of the long duration and the large occupation of memory of the entire processing. For the East façade, it has produced 20,920 points per m^2 with a spacing of 0.7 cm.
In fact, the use of UH could be useful only if the aim is to obtain a detail of a very limited portion of the investigated object by creating a reduced bounding box.

3.4 Procedure validation

The geodetic network has been measured together with the acquisition of the MS scans, as mentioned before. The TLS scans have been pre-processed, oriented and exported using the software supplied by Zoller+Fröhlich. Then, they have been aligned using at least 8 targets and refined using the ICP algorithm. They have been manually edited in CloudCompare (www.cloudcompare.org) to remove outliers and noise due to the vegetation. The coordinates of the TLS targets have been acquired with the MS, resulting in final point clouds directly co-registered in the same reference frame of the UAS Photogrammetry survey.
The generated photogrammetric dense clouds have been validated by comparing them with the reference TLS scan. The comparison has been performed for the O case, considering 15 GCPs and H EO quality. The correspondence between each photogrammetric dense cloud (namely L, M and H dense quality) and the TLS scan has been assigned

considering the shortest Euclidean distance. The computed statistics are shown in Table 5. The points located at distances greater than the 95th percentile have been excluded. In fact, they have been considered outliers due to the presence of the vegetation.

	Low dense cloud quality	Medium dense cloud quality	High dense cloud quality
Average (cm)	-41.2	-3.6	0.5
Standard deviation (cm)	75.3	16.4	3.5
Min (cm)	-167.6	-79.2	-16.9
Max (cm)	140.0	34.4	15.3
RMS (cm)	85.9	16.8	3.6
Sample size (10^6 points)	1.47	8.61	110.08
Outliers (10^3 points)	163.43	956.52	1,223.08

Table 4. Comparison between photogrammetric point clouds to the TLS reference scan

In Figure 8 a graphic representation of the statistics is given. It is quite evident that the increase of the dense cloud processing causes the progressive convergence toward zero of the average, together with a significant reduction of the standard deviation.

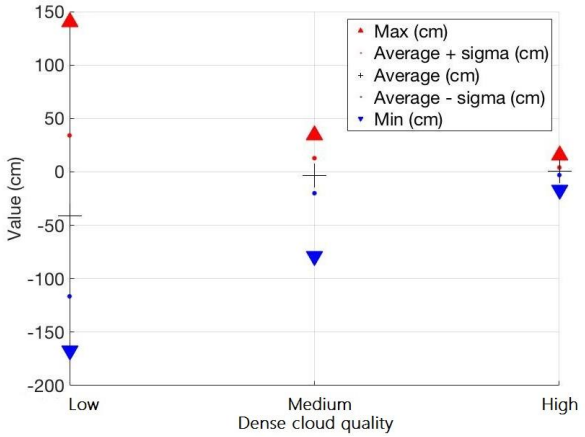

Figure 8. Graphic representation of the statistical value of the comparison between points clouds obtained with photogrammetric approach and the TLS point clouds for the entire structure

In

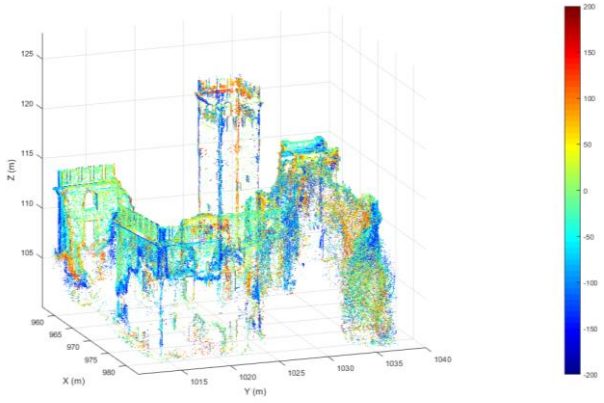

Figure 9, Fig. 10 and Fig. 11 the UAS photogrammetric point clouds realized with different quality (L, M and H respectively) are shown. The colour scale represents the Euclidean distance with respect to the reference TLS scan, expressed in centimetres.

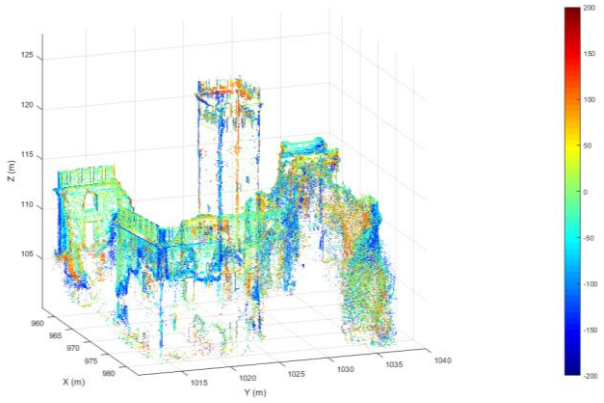

Figure 9. Differences (in centimetres) between the UAS point clouds with low dense cloud quality and the TLS point clouds for the Castle of Casalbagliano

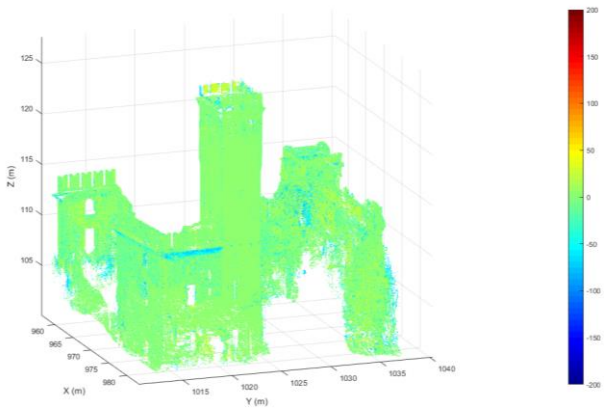

Figure 2. Differences (in centimetres) between the UAS point clouds with medium dense cloud quality and the TLS point clouds for the Castle of Casalbagliano

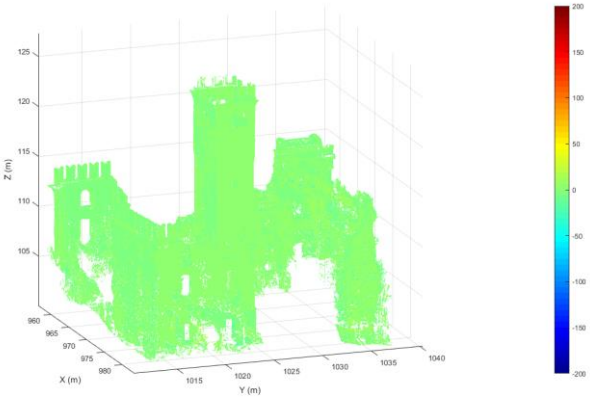

Figure 31. Differences (in centimetres) between the UAS point clouds with high dense cloud quality and the TLS point clouds for the Castle of Casalbagliano

Despite the L dense cloud can be built even on-site in few minutes, it produces a not satisfactory result for any metric application. Fig. 9, Fig. 10 and Fig. 11 show that an increment of the image quality reflects in an increment of the point cloud density, resulting in a more detailed description of the investigated object. Furthermore, the conducted analysis shows that, starting from M quality, it is possible to use the generated 3D data for a preliminary evaluation of the volumes and the dimensions of the structures, with an accuracy in the order of few centimetres.
Considering that the time for creating the points cloud in M is 1.5 hours, whereas it is about 11 hours for H, a dense cloud generation in M is suggested for the overall structure assessment. On the other hand, an H processing is suggested only for those portions of the structure whose analyses require a higher amount of details.

4. DATA DISTRIBUTION

Once the final products are obtained, the issue of data distribution has to be considered. Often, the end-users are not able to manage the final outputs. Dealing with 3D models and point clouds requires several skills, including data formats, the use of specific software and knowing how to retrieve derived information from models (e.g. measurements, sections, colour values, etc.) and how to manage data typically characterized by enormous sizes. In this regard, hardware with certain specifications and performances (e.g. processor, RAM, graphic card, etc.) are necessary to better handle this kind of data.
For these reasons, the outputs delivered to the end-users are usually 2D products, like plans, sections, orthophotos and Digital Elevation Models (DEMs), which are easier to manage with the most commonly used Computer-Aided Drafting (CAD) software and Geographical Information System (GIS) applications. This leads to an inevitable loss of related information given by the nature of the survey itself (e.g. colours, precision, resolution, etc.)
Moreover, in case of emergency, sharing simultaneously the results with all the institutions and operators involved can be very useful to accelerate the data distribution and the operations. Web publication of 3D models and point clouds allows users to easily navigate, query and analyse 3D data without requiring any specific skills.
For all these reasons, a Web-based approach has been chosen and tested.

4.1 Web publication

Thanks to recent software and hardware advancements, dealing with 3D products on Web is easier and it permits a widespread and simple distribution of the survey results.
The Web publication of high-resolution models and point clouds has been tested using two different and well-known tools: 3D Heritage Online Presenter (3DHOP) and Potree. The former (http://vcg.isti.cnr.it/3dhop/) has been developed by the research group of the Visual Computing Lab of ISTI-CNR (Pisa, Italy), and it is a software framework for the creation of interactive Web presentation of high-resolution 3D models. The latter (http://potree.org/) has been developed at the Institute of Computer Graphics and Algorithms of Technische Universität (Vienna, Austria), and it is a Web-based renderer for large point clouds. Both are free and open source packages, which provide ready-to-use components and functions for the Web visualisation of 3D data. These characteristics, combined with the possibility of properly customizing the resulting Web page with basic programming knowledge, are the reasons why these two tools have been chosen for testing.
3DHOP (Potenziani et al., 2015) is based on the WebGL subset of HTML5 and on SpiderGL, a Javascript library for advanced computer graphic programming. It is cross-platform and works on the most common browser (e.g. Google Chrome, Mozilla Firefox, Internet Explorer, Safari and Opera) without the need of additional plugins.
Potree (Schuets, 2016) is WebGL-based and it also works on the most known browsers without the need to install third-party applications.
Both 3DHOP and Potree are based on multi-resolution data structure, which is generally composed by different chunks with different levels of detail. The multi-resolution approach makes the Web visualization faster, but it requires a pre-processing phase for models and point clouds.
Both 3DHOP and Potree provide their own executable to convert single-resolution data into their specific multi-resolution file formats, ready to be published on Web. By default, 3DHOP provides many tools for a basic navigation of the model, while other ready-to-use functions (e.g. sections, measure of distance, clickable hotspots, etc.) can be set, as shown in Fig. 12. In this case, basic programming skills are required but the detailed instructions of the available documentation make this step easier even for unexperienced developers. The framework can be used as a simple viewer if any interaction with the Web page is configured, but it can be connected to other active element of the Web page modifying Javascript and CSS/HTML codes.

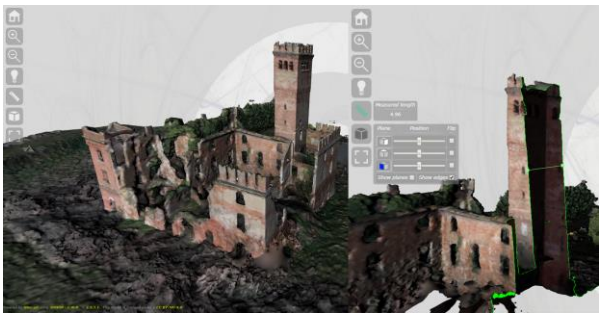

Figure 4. 3D model of the Castel of Casalbagliano published with 3DHOP and examples of some set tools.

About Potree, most of the tools are provided by default resulting in a complex Web viewer. Navigation and measure tools (angles, areas, volumes, distances, etc.), elevation profile and other style functions are available with no configuration, as shown in Fig. 13, while more specific tools (e.g. annotations and overview map) require some changes in the code from the developer. Because of the lack of documentation (only example codes are available), the customization of Potree viewer needs good programming skills.

Figure 5. 3D model of the Castel of Casalbagliano published with Potree and examples of some set tools

Thanks to their Open Source nature, both 3DHOP and Potree Web viewers are characterized by high flexibility, which allows creating customized renderer with different levels of complexity, depending on the developer's programming skills.
In conclusion, these two packages provide a useful and complete instrument for data distribution, simplifying the use of 3D models and point clouds for all involved operators.

5. CONCLUSIONS

In this paper, some guidelines useful for choosing the most suitable operative strategy in case of emergency survey have been delineated. UAS photogrammetry has emerged as the preferable technique in such scenarios, because it allows obtaining high accuracy, reducing at the same time the risks for the operators. Moreover, this technique is fast and cheap, it allows to inspect the object from above and it is characterized by a high efficiency and optimization of resources.
The analysed case study was chosen because it can be assimilated to an emergency scenario. In fact, the real risk of collapse makes the approach of the inner part of the castle impossible.
The impact of different processing parameters has been evaluated (e.g. image acquisition geometry, number and distribution of the GCPs and image quality in the different processing phases) to understand their influence on the final metric accuracy of the delivered 3D models and the impact on the processing time. All the tests have been carried out using Agistoft Photoscan, one of the most common commercial software.
Concerning the requested time for computing the External Orientation (EO) and the dense cloud generation, it has clearly emerged that the number of frames, which composed the images dataset, mainly influences it. In order to optimize this number, it is important to evaluate which point of view can guarantee a full reconstruction of the investigated object, together with the desired GSD.
The number of GCPs is not much influent in terms of processing time for both EO computation and dense cloud generation, but GCPs distribution has to be carefully evaluated. Reducing the amount of GCPs makes the survey operations faster and their detection on the photos by the operator easier. Moreover, the possibility to place the targets could be compromised by the bad state of the site and the inaccessibility of the area. On the other hand, a bad distribution of the GCPs can result in a low quality accuracy of the photogrammetric solution.
The processing quality (i.e. image resolution) should be decided considering the final expected accuracy, as well as the operative conditions. In particular, it is recommended to downscale the image resolution by a factor 4 (medium quality) when it is sufficient to reconstruct the global shape of the investigated structure. Eventually, the images in their full resolution (high quality) can be used only for those areas where a high level of detail is requested.
Finally, some techniques for Web publication have been discussed. The tools 3DHOP and Potree, available as open source software, allow the navigation and the measurement of both 3D models and point clouds. The availability of these platforms could help the operators to better enhance their work, and to disseminate it to the final users, which could easily make use of the published data.

ACKNOWLEDGEMENTS

This work comes from the master thesis of one of the authors. The authors would like to thank for the provided support:

- Comune di Alessandria, in particular Arch. Marco Genovese and Geom. Gianfranco Ferraris, for their availability;
- Soprintendenza belle arti e paesaggio della Provincia di Alessandria, in particular Arch. Luigi Pedrini and Dott. Valentina Uras;
- the co-supervisors of the thesis: Eng. Serena Cattari and Arch. Rita Vecchiattini, respectively at DICCA and DAD Departments at the Genoa University.

REFERENCES

Achille, C., Adami, A., Chiarini, S., Cremonesi, S., Fassi, F., Fregonese, L., Taffurelli, L., 2015. UAV-based photogrammetry and integrated technologies for architectural applications—Methodological strategies for the after-quake survey of vertical structures in Mantua (Italy). *Sensors* 15(7), pp. 15520-15539.

Ballarin, M., Buttolo, V., Guerra, F., Vernier, P., 2013. Integrated surveying techniques for sensitive areas: San Felice sul Panaro. *ISPRS Annals of the Photogrammetry, Remote Sensing and Spatial Information Sciences* 5, W1.

Bruno, F., Bruno, S., De Sensi, G., Luchi, M. L., Mancuso, S., Muzzupappa, M., 2010. From 3D reconstruction to virtual reality: A complete methodology for digital archaeological exhibition. *Journal of Cultural Heritage* 11(1), pp. 42-49.

Brutto, M. L., Garraffa, A., Meli, P., 2014. UAV platforms for cultural heritage survey: first results. *ISPRS Annals of the Photogrammetry, Remote Sensing and Spatial Information Sciences* 2(5), p. 227.

Fagandini, R., Federici, B., Ferrando, I., Gagliolo, S., Pagliari, D., Passoni D., Pinto, L., Rossi, L., Sguerso, D., 2017. Evaluation of the Laser Response of Leica Nova Multistation MS60 for 3D Modelling and Structural Monitoring. *In International Conference on Computational Science and Its Applications*, pp. 93-104

Gagliolo, S., Fagandini, R., Federici, B., Ferrando, I., Passoni, D., Pagliari, D., Pinto, L., Sguerso, D., 2017. Use of UAS for the conservation of historical buildings in case of emergencies. *International Archives of the Photogrammetry, Remote Sensing and Spatial Information Sciences, Vol. XLII-5/W1*, p. 81-88.

Grün, A., Remondino, F., and Zhang, L., 2004. Photogrammetric reconstruction of the great Buddha of Bamiyan, Afghanistan. *The Photogrammetric Record* 19.107, pp. 177-199.

Lague, D., Brodu, N., Leroux, J., 2013. Accurate 3D comparison of complex topography with terrestrial laser scanner: application to the Rangitikei canyon (N-Z). *ISPRS Journal of Photogrammetry and Remote Sensing* 82, pp. 10-26

Meyer, D., Hess, M., Lo, E., Wittich, C. E., Hutchinson, T. C., Kuester, F., 2015. UAV-based post disaster assessment of cultural heritage sites following the 2014 South Napa Earthquake. *Digital Heritage*, Vol. 2, pp. 421-424.

Potenziani, M., Callieri, M., Dellepiane, M., Corsini, M., Ponchio, F., Scopigno, R., 2015. 3DHOP: 3D Heritage Online Presenter. Computers & Graphics, Volume 52, pp. 129-141, ISSN 0097-8493.

Remondino, F., 2011. Heritage recording and 3D modeling with photogrammetry and 3D scanning. *Remote Sensing* 3(6), pp. 1104-1138.

Sauerbier, M., Eisenbeiss, H., 2010. UAVs for the documentation of archaeological excavations. *International Archives of Photogrammetry, Remote Sensing and Spatial Information Sciences* 38 (Part 5), pp. 526-531.

Schuetz, M., 2016. Potree: Rendering large point clouds in Web browser.

Themistocleous, K., Ioannides, M., Agapiou, A., Hadjimitsis, D. G., 2015. The methodology of documenting cultural heritage sites using photogrammetry, UAV, and 3D printing techniques: the case study of Asinou Church in Cyprus. In Third International Conference on Remote Sensing and Geoinformation of the Environment, pp. 953510-953510.

Wojciechowski, R., Walczak, K., White, M., Cellary, W., 2004. Building virtual and augmented reality museum exhibitions. Proceedings of the ninth international conference on 3D Web technology, ACM.

Xu, Z., Yang, J., Peng, C., Wu, Y., Jiang, X., Li, R., Zeng, Y., Gao, Y., Liu, S., Tian, B., 2014. Development of an UAS for post-earthquake disaster surveying and its application in Ms7. 0 Lushan Earthquake, Sichuan, China. *Computers & Geosciences* 68, pp. 22-30.

Yastikli, N., 2007. Documentation of cultural heritage using digital photogrammetry and laser scanning. *Journal of Cultural Heritage* 8.4, pp. 423-427.

Yilmaz, H. M., Yakar, M., Gulec, S. A., Dulgerler, O. N., 2007. Importance of digital close-range photogrammetry in documentation of cultural heritage. Journal of Cultural Heritage 8.4, pp. 428-433.